Title

Gliding motility and polysaccharide secretion in filamentous cyanobacteria

Journal

Molecular Microbiology, 98(6)

ISSN

0950-382X

Authors

Khayatan, Behzad
Meeks, John C
Risser, Douglas D

Publication Date

2015-12-01

DOI

10.1111/mmi.13205

Peer reviewed

Molecular Microbiology (2015) 98(6), 1021–1036 ■
doi:10.1111/mmi.13205
First published online 20 October 2015

Evidence that a modified type IV pilus-like system powers gliding motility and polysaccharide secretion in filamentous cyanobacteria

Behzad Khayatan,[1] John C. Meeks[2] and Douglas D. Risser[1]*
[1]*Department of Biology, University of the Pacific, Stockton, CA 95211, USA.*
[2]*Department of Microbiology, University of California, Davis, CA 95616, USA.*

Summary

In filamentous cyanobacteria, the mechanism of gliding motility is undefined but posited to be driven by a polysaccharide secretion system known as the junctional pore complex (JPC). Recent evidence implies that the JPC is a modified type IV pilus-like structure encoded for in part by genes in the *hps* locus. To test this hypothesis, we conducted genetic, cytological and comparative genomics studies on *hps* and *pil* genes in *Nostoc punctiforme*, a species in which motility is restricted to transiently differentiated filaments called hormogonia. Inactivation of most *hps* and *pil* genes abolished motility and abolished or drastically reduced secretion of hormogonium polysaccharide, and the subcellular localization of several Pil proteins in motile hormogonia corresponds to the site of the junctional pore complex. The non-motile Δ*hpsE-G* strain, which lacks three glycosyltransferases that synthesize hormogonium polysaccharide, could be complemented to motility by the addition of medium conditioned by wild-type hormogonia. Based on this result, we speculate that secretion of hormogonium polysaccharide facilitates but does not provide the motive force for gliding. Both the Hps and Pil homologs characterized in this study are almost universally conserved among filamentous cyanobacteria, with the Hps homologs rarely found in unicellular strains. These results support the theory that Hps and Pil proteins compose the JPC, a type IV pilus-like nanomotor that drives motility and polysaccharide secretion in filamentous cyanobacteria.

Accepted 3 August, 2015. *For correspondence. E-mail drisser@pacific.edu; Tel. 2099322953; Fax 2099463022.

Introduction

The ability to translocate across a solid surface in the absence of flagella, often referred to as gliding or twitching motility, is a common trait among many different bacteria. The means of propulsion, however, differ substantially. One of the most well-studied forms of surface motility is the twitching motility of proteobacteria such as *Myxococcus xanthus*, which is driven by the retraction of type IV pili (T4P) following extension and adherence to the substratum or a neighboring cell (Merz *et al.*, 2000; Skerker and Berg, 2001). Several other forms of T4P-independent surface motility have also been defined to varying degrees, including the presence of a second gliding motor in *M. xanthus*, and various mechanisms in *Flavobacteria*, and *Mycoplasma* to name a few (for review, see Jarrell and McBride, 2008).

Many species of cyanobacteria are also capable of surface motility. In both unicellular and filamentous strains, surface motility enables phototaxis behavior to seek out favorable light environments (Castenholz, 1982). In filamentous cyanobacteria, motility facilitates additional functions including the development of supracellular structures such as colonial aggregates and reticulates thought to be evident in fossil records (Shepard and Sumner, 2010; Risser *et al.*, 2014), and the establishment of nitrogen-fixing symbioses with plants and fungi in certain heterocyst-forming strains (Kluge *et al.*, 2003; Meeks, 2006). In many heterocyst-forming strains, only transiently differentiated filaments termed hormogonia are capable of motility (Rippka *et al.*, 2001). The most extensively defined cyanobacterial surface motility, that of the unicellular cyanobacterium *Synechocystis* sp. strain PCC 6803 (herein *Synechocystis*), appears to be facilitated by T4P in a manner analogous to the twitching motility of *M. xanthus* (Bhaya *et al.*, 2000). In contrast, the motor driving motility in filamentous cyanobacteria is not well defined.

Based on observational studies, including a number of ultrastructure analyses, three distinct theories have been proposed to account for motility in these organisms. The first proposes that secretion of a polysaccharide slime provides the motive force. Some of the earliest observations of filamentous cyanobacteria found that gliding

filaments emanate slime at the septal junctions (Walsby, 1968). Subsequently, a putative polysaccharide secretion system termed the junctional pore complex (JPC) was identified by ultrastructure studies (Hoiczyk and Baumeister, 1998). These structures are arranged in rings adjacent to the septal junction in several species of cyanobacteria and posited as the polysaccharide-secreting gliding motor, but the identity of the proteins that comprise this apparatus were not identified. A recent study using *in situ* atomic force microscopy demonstrated a positive correlation between the rate of gliding and the thickness of polysaccharide deposition in hormogonia of *Nostoc punctiforme*, lending further support to this theory (Dhahri *et al*., 2013). A second theory postulates that contraction waves driven by contractile fibers provide the motive force. Evidence in support of this theory is limited to a handful of conflicting ultrastructure studies that found various fibrils either internal or external to the outer membrane in several strains of filamentous cyanobacteria (Halfen and Castenholz, 1970; Hoiczyk and Baumeister, 1995; Adams *et al*., 1998; Read *et al*., 2007). The third theory holds that like *Synechocystis*, T4P provide the motive force. This theory is supported by three studies on the ultrastructure of hormogonia from *Calothrix* and *Nostoc* spp., which reported the presence of peritrichous pili on the surface of putative motile hormogonia (Dick and Stewart, 1980; Damerval *et al*., 1991; Duggan *et al*., 2007). In one of these studies, four T4P system homologs were genetically inactivated, including a putative pseudopilin/minor pilin, prepilin peptidase and two PilT-like pilus retraction proteins, but their role in motility was inconclusive because the parent strain used for mutant construction did not display robust motility (Duggan *et al*., 2007). Yet, in most other motile filamentous cyanobacteria examined, pili have not been observed. These discrepancies led to the suggestion that, within the filamentous cyanobacteria, different mechanisms for motility may exist (Adams, 2001).

More recent genetic and molecular studies have begun to identify the genes that encode proteins for motility in the model filamentous cyanobacterium *N. punctiforme*. These genes include: (i) the *hmp* locus, which encodes for chemotaxis-like proteins required for transcriptional activation of *hps* genes, and (ii) the *hps* locus, which encodes for glycosyl transferases, proteins with homology to pseudopilins or minor pilins found in type II secretion (T2S) and T4P systems respectively, and uncharacterized membrane proteins that are unique to filamentous cyanobacteria (Risser and Meeks, 2013; Risser *et al*., 2014). This led to speculation that the JPC is a modified T4P-/T2S-like system encoded for, at least in part, by the *hps* locus. Further support for this possibility came with the discovery that the putative major pilin in *N. punctiforme* localizes to rings at the septal junctions (Risser *et al*., 2014). In order to provide additional evidence for or against this model, we conducted genetic, cytological and comparative genomics analyses of Hps and T4P proteins encoded in the *N. punctiforme* genome. The results presented here are consistent with the theory that the junctional pore complex is a modified T4P-/T2S-like system that powers gliding motility and polysaccharide secretion in filamentous cyanobacteria.

Results

A T4P-like system is essential for motility in N. punctiforme

To conclusively determine the role of a T4P-like system in gliding motility of hormogonia, differentiated motile filaments, of *N. punctiforme*, in frame deletions were constructed in the genes for several T4P homologs known to be essential for T4P function and motility in other organisms. Gene names are designated based on the standard nomenclature suggested by Melville and Craig (2013). For gene maps, and a list of the locus tags, gene names, and functions for Hps proteins and putative T4P homologs in *N. punctiforme* see Fig. S1 and Table S1, and a review of T4P function by (Giltner *et al*., 2012). Genes targeted for in frame deletions were those encoding for the putative major pilin protein, PilA, pilus extension ATPase, PilB, pilus retraction ATPases, PilT1 and PilT2, and the outer membrane secretin PilQ, as well as the pseudopilin/minor pilin, HpsH; the phenotypes of the deletion strains were assayed via both plate and time-lapse motility assays along with previously constructed strains harboring deletions within the *hps* locus. Deletion of *hpsA*, *hpsB-D*, *hpsE-G*, *pilA*, *pilB*, *pilT1* or *pilQ* completely abolished motility as evidenced by both plate (Fig. 1A) and time-lapse motility assays (SMOV1). Deletion of *hpsH*, *hpsJ* and *pilT2* decreased the extent of movement from the source to varying degrees relative to the wild-type in plate motility assays (Fig. 1A and B). For these strains, the rate of motility was quantified using time lapse microscopy (Fig. 1C, SMOV2-5). The majority of hormogonia for the Δ*hpsH*- and Δ*hpsJ*-strains were motile, but slower than wild-type hormogonia. In contrast, the majority of hormogonia for the *pilT2*-deletion strain were non-motile during the 30 min time lapse assays and often individual hormogonia would either start or stop moving during the assays. For those hormogonia that were motile, the rate of motility was significantly decreased compared with the wild type (Fig. 1C).

In *Synechocystis*, PilT2 is dispensable for motility, but a *pilT2*-null mutant displayed negative rather than positive phototaxis in response to a directional light source (Bhaya *et al*., 2000). In contrast, the *N. punctiforme* Δ*pilT2* strain retained positive phototaxis, as did the two *hps*-deletion

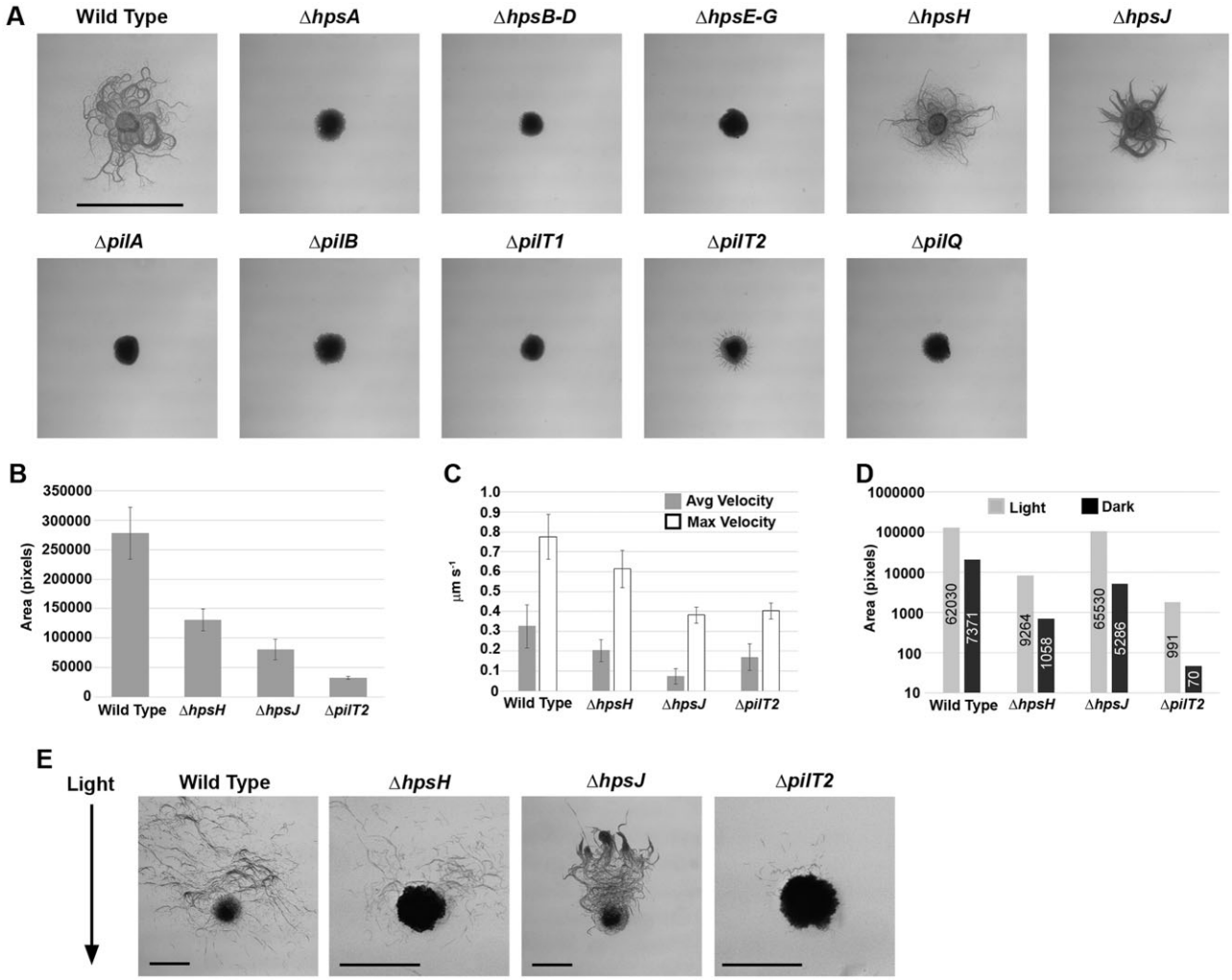

Fig. 1. Hps and Pil proteins are essential for motility in *N. punctiforme*.
A. Light micrographs taken with a dissecting microscope of plate motility assays, strains as indicated. Bar = 5 mm.
B. Quantification of colony spreading from plate motility assays ($n = 3$, error bars = 1 SD).
C. Quantification of velocity for individual hormogonium filaments (measurements represent the mean of the average from three biological replicates with the following number of hormogonia quantified for each strain for each replicate: wild-type $n_1 = 37$, $n_2 = 50$, $n_3 = 17$; Δ*hpsH* $n_1 = 24$, $n_2 = 46$, $n_3 = 24$; Δ*hpsJ* $n_1 = 26$, $n_2 = 26$, $n_3 = 26$, Δ*pilT2* $n_1 = 7$, $n_2 = 21$, $n_3 = 7$).
D. Quantification of phototactic response. Areal values are depicted on log scale due to the high variation in motility between strains ($n = 3$, number inside bars = 1 SD).
E. Light micrographs taken with a dissecting microscope of phototaxis assays. Direction of light as indicated, bar = 1 mm.

mutants that retained motility, Δ*hpsH* and Δ*hpsJ*. (Fig. 1D and E). Negative phototaxis has not been detected in wild-type hormogonia of *N. punctiforme*, even under 500 μmoles photons/m^2/s (Campbell *et al.*, 2015). The results from analysis of these mutant strains clearly demonstrate the necessity of a T4P-like system for motility in *N. punctiforme*.

Deletion of hps and pil genes affects localization of PilA

To assess the role of *hps* and *pil* genes in the synthesis and expression of PilA on the surface of hormogonia, PilA was assayed via immunoblot analysis and immunofluorescence in each of the *hps*- and *pil*-deletion strains (Fig. 2, Fig. S2). PilA was undetectable by immunoblotting or immunofluorescence in the Δ*pilA* strain, which served as a negative control to confirm the specificity of the α-PilA antibody. PilA was detectable by immunoblot analysis for all of the remaining strains confirming that none of the mutations prevented synthesis of PilA, but the Δ*hpsB-D* and Δ*hpsH* strains, which encode for minor/pseudopilins, consistently displayed lower levels of PilA than the wild-type, perhaps due to a feedback mechanism that normally maintains a proper ratio of PilA to minor/pseudopilin. In the Δ*pilB* and Δ*pilQ* strains, PilA was detectable via immunoblotting, but not by

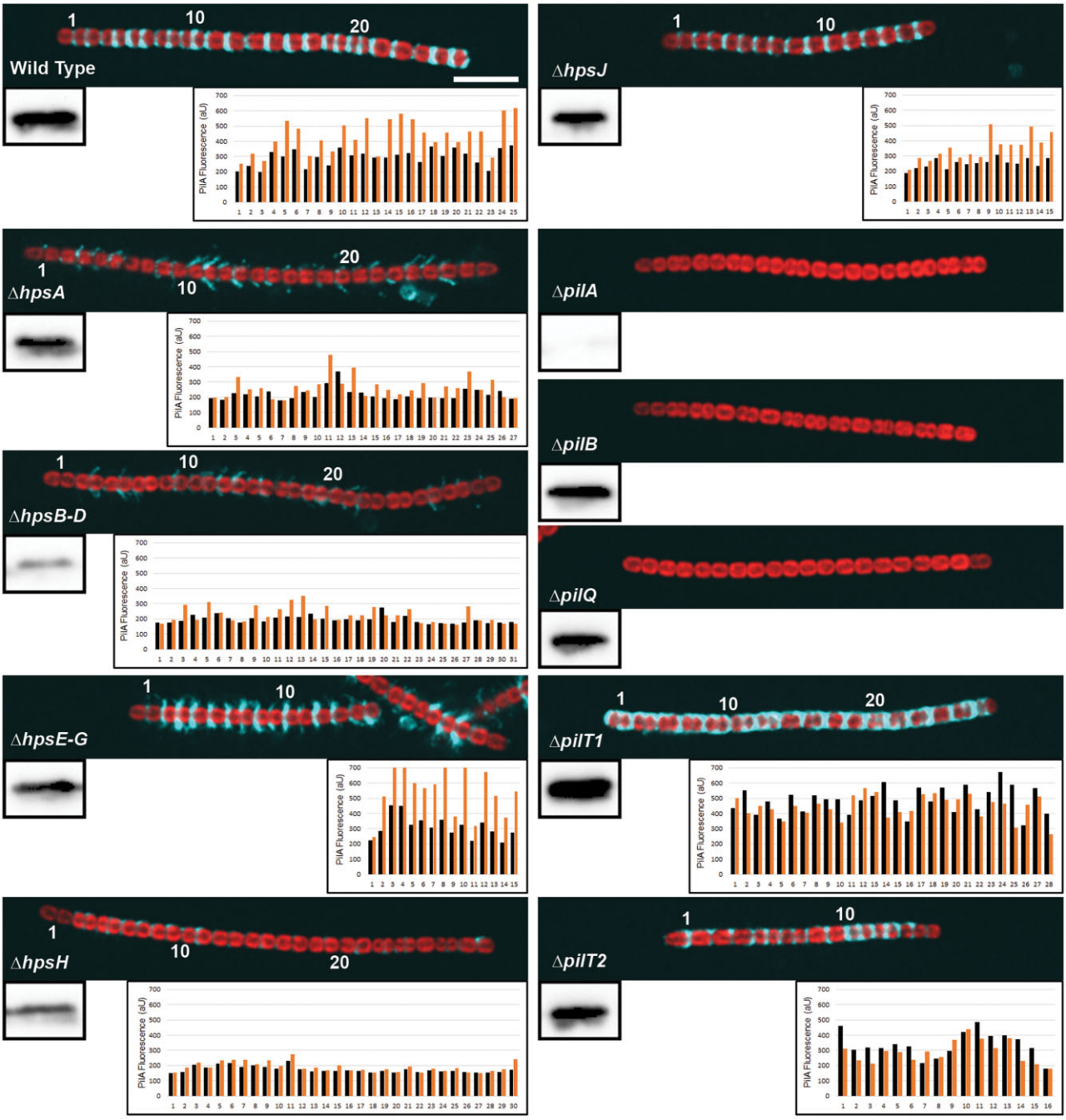

Fig. 2. PilA synthesis and localization in *hps*- and *pil*-deletion strains. Merged images from fluorescence micrographs for PilA immunofluorescence (cyan) and autofluorescence (red) are depicted for a hormogonium from each strain as indicated. Bar = 10 μm. For each image, a panel on the lower left depicts the results from immunoblot analysis of whole cell PilA and the graph on the lower right depicts quantification of the PilA-immunofluorescent signal on each side of a septal junction. The numbers on the *x*-axis correspond to the septal junctions as indicated by reference numbers in the fluorescent micrograph. Black and orange bars depict the fluorescent signal to the left and right of each junction respectively.

immunofluorescence. This is consistent with the function of PilB and PilQ as the pilus extension ATPase and outer membrane secretin, respectively, and also demonstrates that the immunofluorescence protocol employed here detects only PilA that has exited the outer membrane. In wild type hormogonia, PilA localized to the septal junction as previously reported (Risser *et al.*, 2014) and displayed a consistent polarity to one side of each septum throughout the filament. In order to confirm this apparent polarity, the fluorescent signal derived from PilA in cells adjacent to

each side of each septum was quantified. This quantitative analysis confirmed the consistent, biased localization of PilA to one side of the septal junctions throughout a hormogonium filament. Hormogonia of both the Δ*hpsH* and Δ*hpsJ* strains displayed PilA localization and filament polarity similar to the wild type, although the amount of PilA expressed on the surface was reduced in the Δ*hpsH* strain, consistent with the results from immunoblotting, and implying that a reduction in PilA may partially account for the decreased rate of motility for this strain.

The surface of hormogonia for the Δ*pilT1* strain accumulated high levels of PilA. Although PilA was not typically equivalent on either side of an individual septal junction, there was no apparent co-ordinated polarity throughout a hormogonium and the level of PilA on both sides of junctions was usually high. These results support an essential role for PilT1 in pilus retraction; one possible explanation for these results would be that the co-ordinated polarity of PilA to one side of the septa in wild-type hormogonia is the result of a co-ordinated increase in PilT1 activity at one pole of the cells. Unlike deletion of *pilT1*, deletion of *pilT2* did not result in increased levels of PilA on the surface of hormogonia. Individually, some septal junctions displayed polar localization of PilA similar to wild-type hormogonia, whereas other junctions appeared to lack a polar bias and overall, the co-ordinated polarity among cells of the filament was lost.

The *hpsA*, *hpsB-D* and *hpsE-G* deletion strains synthesized and expressed PilA to varying levels at the septal junctions but with a marked change in appearance. For each of these strains, PilA protruded out and away from the filament rather than adhering close to the surface. The localization of PilA was clearly biased to one side of the septal junction consistently throughout the filaments, presumably due to extrusion of PilA from only one side of each cell along the filament. The co-ordinated polarity of PilA even in non-motile hormogonia implies that this biased localization pattern precedes motility and cannot be explained simply as the result of a dragging effect on PilA as filaments move.

The immunofluorescent localization of PilA to the septal junction reported here differs substantially from the peritrichous arrangement of pili previously reported for hormogonia of *N. punctiforme* (Duggan *et al*., 2007). One hypothesis that could account for this discrepancy posits that, as filaments transition from motile hormogonia to sessile primordia and then vegetative filaments, the localization pattern of PilA may change. To test this hypothesis, PilA localization was visualized between 24 and 168 h after the induction of hormogonia (Fig. 3). Forty-eight hours post induction, which corresponds to the time when hormogonia cease motility, filaments began to resemble the Δ*pilT1* strain by displaying intense accumulations of PilA that emanated from the septal junctions, but that

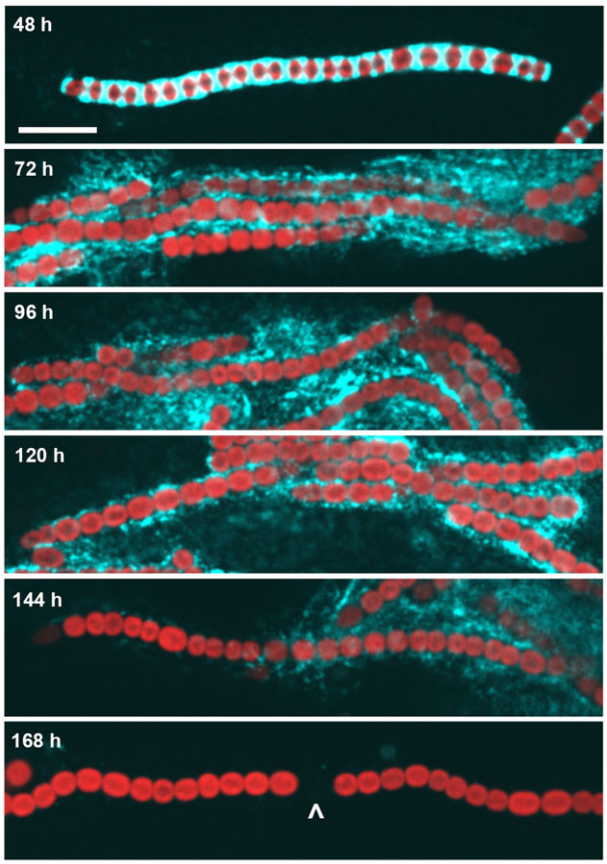

Fig. 3. Changes in PilA presence and localization over time as hormogonia revert to a non-motile vegetative state. Merged images from fluorescence micrographs for PilA immunofluorescence (cyan) and autofluorescence (red) is depicted for wild-type filaments at various times (as indicated) after the induction of hormogonia. Caret in bottom panel indicates a heterocyst, which lacks phycobiliprotien-induced fluorescence, in the reversion to the mature vegetative state. Bar = 10 μm.

lacked obvious directionality. By 72 h, localization of PilA to the septal junctions dissipated; rather, diffuse fluorescence was observed around filaments. At this point, it was difficult to find isolated filaments as they tended to adhere to one another. This localization pattern was maintained between 72 and 144 h post induction, whereas the intensity of the fluorescent signal dissipated with time. Seven days post induction, vegetative filaments lacking any signs of PilA localization were observed and the filaments contained distinct heterocysts. These observations are consistent with a switch in the localization pattern from the septal junctions in motile hormogonia to either a peritrichous arrangement or a loose association of released PilA in sessile primordia. In the latter two cases, the pili are probably important for adhesion as filaments transition to the sessile state and it is likely that these filaments, not motile hormogonia, were observed in previous studies. The mechanism that facilitates the change in PilA localization is unknown at this point.

Subcellular localization of type IV pilus and Hps locus proteins

Based on the results from the immunofluorescence studies of PilA, we would expect Hps and Pil proteins to localize to the cell poles in hormogonia. To determine the subcellular localization of various Hps and Pil proteins, the chromosomal alleles for *hpsA*, *hpsE*, *hpsH*, *hpsJ*, *pilB*, *pilT1* and *pilT2* were replaced with *gfp*-tagged variants. Although strains harboring *gfp*-tagged *hpsA*, *hpsE* and *hpsH* were all motile to varying degrees, GFP could not be detected either by fluorescence microscopy or immunoblot analysis, indicating that these proteins are expressed at low levels, or that the GFP tag is unstable (Fig. S3A and B). Strains harboring *gfp*-tagged *hpsJ*, *pilB*, *pilT1* and *pilT2* produce observable fluorescent signals and a single band corresponding to the predicted size for the GFP-tagged proteins was detectable by immunoblot analysis (Fig. S1B). The motility and phototaxis properties of the *hpsJ*-, *pilT1*- and *pilT2-gfp* strains were similar to the corresponding deletion strains, indicating that the *gfp*-tagged proteins encoded by these alleles are non-functional. In contrast to the Δ*pilB* strain, the *pilB-gfp* strain was motile (approximately 50% of wild-type levels in plate motility assays) and displayed positive phototaxis, indicating that PilB-GFP is functional (Fig. S3A and C). Localization of HpsJ was observed in discrete foci around the periphery of the cell but lacked any obvious polarity. It is possible that this is the natural localization of HpsJ; however, this pattern is also reminiscent of proteins that are targeted for degradation and, thus, may be the result of targeting this non-functional protein for destruction (Fig. 4A) (Risser and Callahan, 2009). PilB-, PilT1- and PilT2-GFP localized to discrete bands at both cell poles with no apparent bias for one pole over the other (Fig. 4A). PilB-GFP also accumulated in occasional bright foci that were always localized to the cell poles, especially at the filament termini. The localization of GFP-fused PilT1, PilT2 and PilB correlates with the localization of PilA by immunofluorescence and does not support the idea that peritrichous T4P are present in motile hormogonia.

In both *M. xanthus* and *Synechocystis*, the direction of motility corresponds to the asymmetric localization of PilB at the leading pole of motile cells (Bulyha *et al*., 2009; Schuergers *et al*., 2015). Because PilB-GFP was both functional and detectable, we used time lapse assays to observe the localization of PilB-GFP in motile hormogonia (Fig. 4B and SMOV6). The temporal interval between capturing the PilB-GFP and red autofluorescence signals, coupled with the speed at which hormogonia move, resulted in some misalignment between the red autoflourescence and PilB-GFP fluorescent signal, and caused some blurring of the fluorescence signal, which prevented us from resolving discrete bands of fluorescence at some junctions. However, many septa displayed a clear bipolar localization pattern for PilB in motile hormogonia and PilB often accumulated at the filament termini for both the leading and lagging ends of filaments (Fig. 4B and C). This result implies that PilB maintains a symmetric bipolar localization as hormogonia move. Consistent with this, there was no obvious change in the localization of PilB-GFP as a hormogonium reversed direction; a clear bipolar localization of PilB-GFP could be observed for some septa both prior and subsequent to a reversal (Fig. 4B and C). To provide some confirmation that there was no dynamic, asymmetric localization of PilB-GFP corresponding to the direction of motility, the fluorescent signal from PilB-GFP along the length of the filament was quantified, and the average fluorescent plot profile for the four time points before and after a reversal were superimposed (Fig. 4D). The polar accumulation of PilB-GFP at the terminus of the lagging pole was used as a reference point to align the plots because it clearly remained static upon reversal. If PilB-GFP accumulated asymmetrically to one side of septa in correlation to the direction of movement, this would be observed as a spatial displacement of the fluorescent peaks before and after a reversal. In contrast, if there is no change in the localization of PilB the fluorescent peaks should be in alignment both before and after a reversal. We observed the later, confirming that there is no dynamic rearrangement of PilB-GFP upon reversal. Because the PilT1- and PilT2-GFP fusions are non-functional, we cannot conclusively determine whether their localization is static or dynamic.

Secretion of a putative hormogonium polysaccharide is dependent on T4P and Hps proteins, but plays a passive role in motility

In *M. xanthus*, T4P-mediated twitching motility requires the presence of polysaccharides produced by the bacteria, which provide a substrate for attachment of the pilus prior to retraction (Li *et al*., 2003). In contrast, it has been proposed that the secretion of polysaccharide itself provides the motive force for gliding in filamentous cyanobacteria (Hoiczyk and Baumeister, 1998), in which case, exogenous addition of polysaccharide would not be sufficient to restore motility in polysaccharide-deficient mutants. In a first step to distinguish between these two models for the motility of *N. punctiforme*, we tested the ability of conditioned medium from cultures containing wild-type hormogonia to complement colonies of non-motile *hps*- and *pil*-deletion strains. Only the Δ*hpsE-G* strain, in which three contiguous genes encoding for glycosyltransferases have been deleted, could be complemented in this manner (for the Δ*hpsE-G* strain see

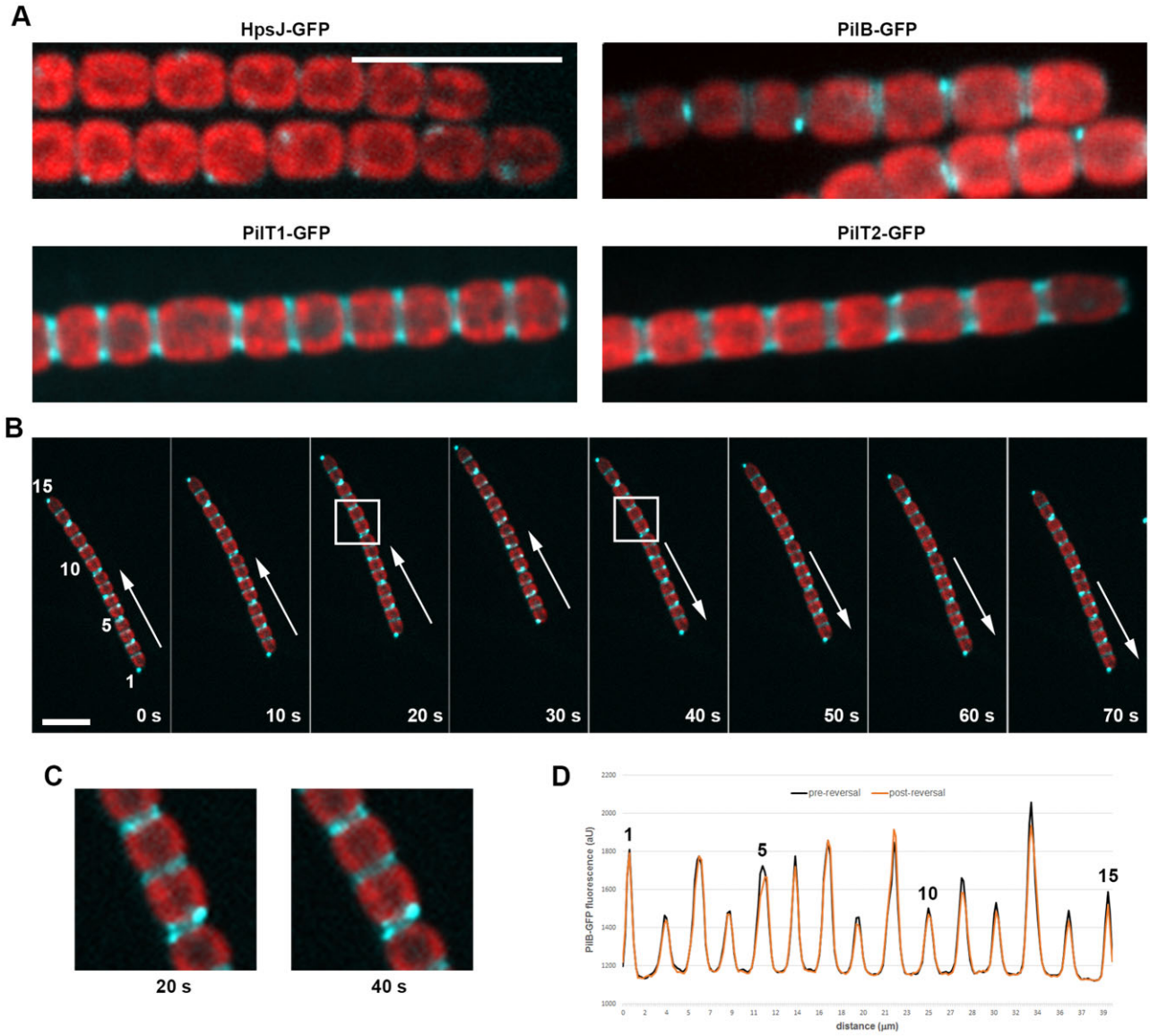

Fig. 4. Subcellular localization of GFP-tagged Hps and Pil proteins.
A. Merged images from fluorescence micrographs for GFP (cyan) and autofluorescence (red) of strains as indicated. Bar = 10 μm.
B. Merged fluorescent images (as described in A) of a motile hormogonium from the *pilB-gfp* strain taken at 10 s intervals as indicated (also depicted in SMOV6). Arrows indicate direction of movement, a reversal occurs between 30 and 40 s. Bar = 10 μm.
C. Inset indicated with white box in B magnified 4×.
D. Quantification of positional fluorescent intensity derived from PilB-GFP before and after a reversal. Depicted is the average plot profile for the four 10 s intervals before (black line) and after (orange line) a reversal. Numbered fluorescent peaks in the plot profile correspond to positions indicated by numbers in B.

Fig. 5A and for the remaining non-motile strains see Fig. S4A).

To quantify the amount of complementing factor, which we speculate is a hormogonium derived polysaccharide that is at least partially assembled by HpsE, F and G, and secreted into the media by various *hps*- and *pil*-deletion strains, we spotted conditioned medium from each strain onto colonies of the Δ*hpsE-G* strain and assessed the ability to restore motility by quantifying colony spreading (Fig. 5A and B). Conditioned medium from the Δ*hpsE-G* strain was never able to complement itself and served as a negative control. Conditioned medium from the Δ*hpsJ* strain displayed the most robust complementation, approximately 2.5-fold that of the wild-type strain, consistent with previous reports that this strain overproduces a hormogonium polysaccharide (Risser and Meeks, 2013). Complementation with conditioned medium from the Δ*hpsH* and Δ*pilT2* strains occurred consistently, but was

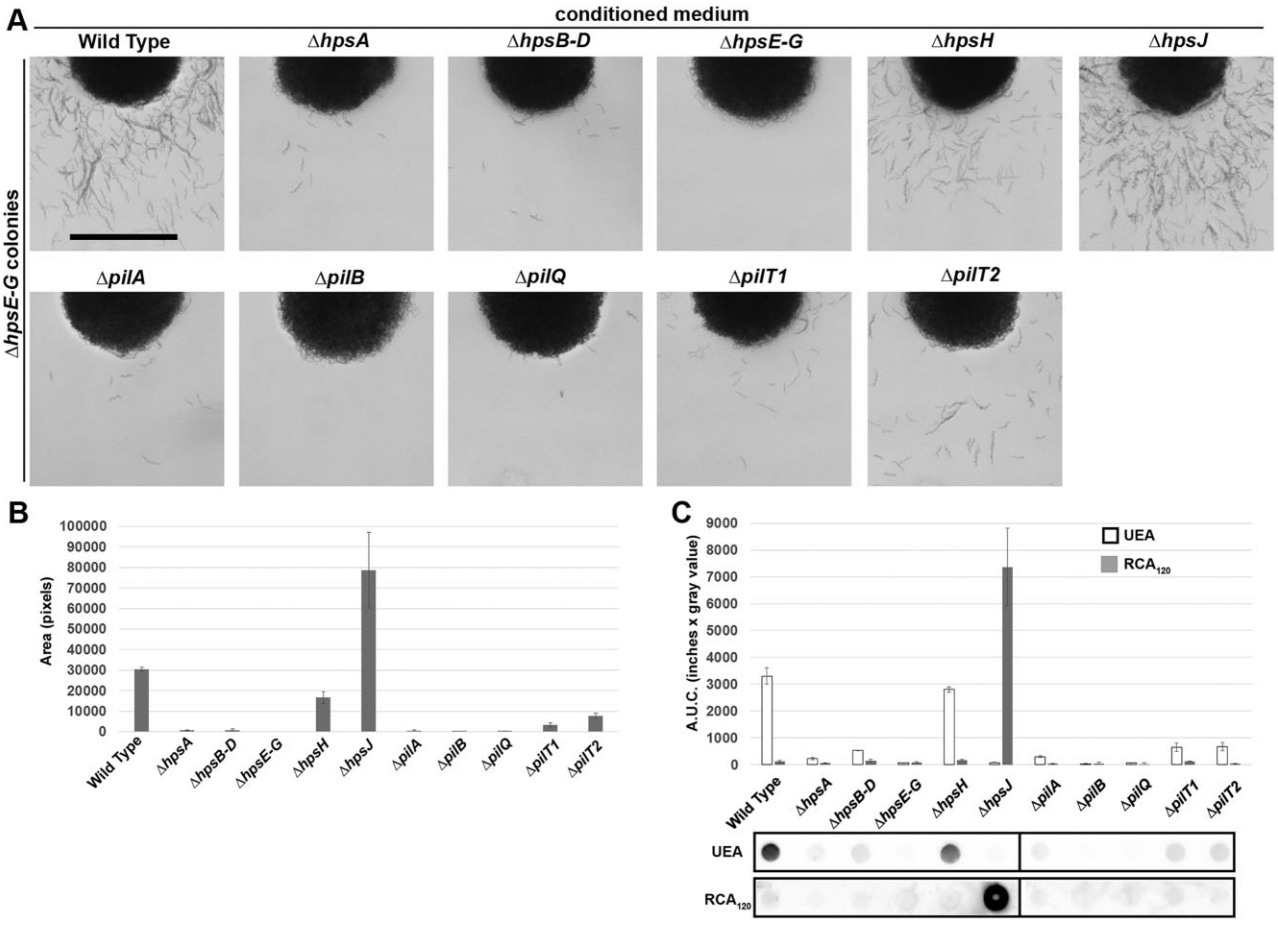

Fig. 5. Exogenous complementation of the Δ*hpsE-G* strain and quantification of hormogonium-polysaccharide.
A. Light micrographs taken with a dissecting microscope and (B) quantification of colony spreading ($n = 3$, error bars = 1 SD) for colonies of the Δ*hpsE-G* strain 72 h after the addition of conditioned medium from various *hps*- and *pil*-deletions strains (as indicated). Bar = 1 mm.
C. Quantification and representative images for lectin blot analysis of hormogonium polysaccharide with UEA and RCA_{120} (as indicated) (A.U.L. = area under the curve, $n = 3$, error bars = 1 SD).

less robust than of the wild type (approximately 50% and 25% of wild-type respectively). Complementation with conditioned medium from the non-motile Δ*pilT1* strain was low, approximately 10% of the wild-type strain, and occasionally assays failed to show any signs of complementation. Conditioned medium from any of the other non-motile strains, Δ*hpsA*, Δ*hpsB-D*, Δ*pilA*, Δ*pilB* and Δ*pilQ* inconsistently showed signs of restoring motility, with the Δ*pilB* and Δ*pilQ* strains only rarely showing any complementation. For these strains, low levels of hormogonium filaments were observed to have migrated out of the colony in some assays (examples of this can be seen in Fig. 5A).

To provide further evidence that the complementing factor is a polysaccharide, lectin blotting was employed. Conditioned medium from the Δ*hpsJ* strain produced high levels of a RCA_{120} specific polysaccharide. This is consistent with previous reports that hormogonia of the Δ*hpsJ* strain overproduce an RCA_{120} specific polysaccharide, and correlates with the robust activity of this medium in the complementation assays. However, with the exception of the Δ*hpsJ* strain, the level of RCA_{120} specific polysaccharide in the conditioned medium did not correlate well with the results from the complementation assays. Subsequently, a number of different lectins were tested for the ability to detect polysaccharides in the conditioned medium. One of these, UEA, detected a polysaccharide in quantities that corresponded closely with the results from the complementation assays (Fig. 5C). This observation is consistent with the hypothesis that the complementing factor present in the conditioned medium is a polysaccharide and indicates that deletion of *hpsJ* causes a change in the composition of the hormogonium polysaccharide, as well as an increase in abundance.

To maximize the dissolution of the putative hormogonium polysaccharide for these assays, we provided agitation by pipetting each hour between 18 and 24 h post-induction of hormogonia to disrupt the clumps of filaments

that form in strains that retain motility. When cultures were treated in this manner, RCA_{120}-specific staining of the hormogonium polysaccharide was detected by fluorescence microscopy only for cultures of the Δ*hpsJ* strain and not for the wild-type or any of the other *hps*- or *pil*-deletion strains (Fig. S4B). Previously, in samples not subject to the rigorous agitation, we were able to detect RCA_{120}-fluorescein stained material in association only with wild-type and Δ*hpsJ* strains; substantially more material was also associated with the Δ*hpsJ* strain (Risser and Meeks, 2013). The latter result was confirmed in this study (Fig. S4B). In contrast, UEA-specific staining was detected by fluorescence microscopy for the wild-type and several of the mutant strains (Fig. S4B). The wild-type strain accumulated high levels of both surface associated and released UEA-specific polysaccharide (Fig. S4B). The Δ*hpsH* and Δ*pilT2* strains also accumulated both surface associated and released UEA-specific polysaccharide, but at lower levels than the wild type. The Δ*hpsA*, Δ*hpsB-D*, Δ*pilA* and Δ*pilT1* strains only accumulated low levels of surface associated UEA-specific polysaccharide. The Δ*hpsE-G*, Δ*hpsJ*, Δ*pilB* and Δ*pilQ* strains did not produce any detectable UEA-specific polysaccharide (Fig. S4B). These results are consistent with the results from both the Δ*hpsE-G* strain complementation assays, and the lectin blot analysis of soluble polysaccharide in the culture medium, and, thus, rule out the possibility that the difference between strains could be attributed to failure of the polysaccharide to dissolve into the medium. Taken together, these results imply that the role of hormogonium polysaccharide in motility is passive but that efficient translocation of the hormogonium polysaccharide out of the cell is dependent on the function of Hps and T4P proteins.

Conservation of the Hps and Pil proteins in filamentous cyanobacteria

It is plausible that distinct motility mechanisms could have evolved independently in various clades of filamentous cyanobacteria and that these organisms do not share a common motility system. Alternatively, a common mechanism may be employed by most, if not all filamentous cyanobacteria. We previously reported that the *hps* locus is conserved among filamentous cyanobacteria, providing support for a common motility system (Risser and Meeks, 2013). Recently, the genome coverage for cyanobacteria was greatly expanded (Shih *et al*., 2013). To comprehensively assess the conservation of components of the *N. punctiforme* motility system in other cyanobacteria, we queried the genomes of 120 cyanobacteria, using *N. punctiforme* Hps and Pil proteins and compiled a database of blast scores for the best hit homolog from each strain. The results are depicted in the form of a heat map (Fig. 6A–C). This expanded analysis confirms the high conservation of the Hps proteins, primarily in filamentous cyanobacteria. The majority of the Hps proteins are absent from the genome of well-studied *Synechocystis*. Unicellular strains that appear to have recently descended from filamentous ancestors (indicated by red arrows in Fig. 6B) typically show a greater conservation of Hps proteins compared with other unicellular strains but less than their filamentous counterparts. This observation implies that reversion from a filamentous to unicellular state relieves selective pressure to maintain the *hps* locus, resulting in a concomitant loss of *hps* genes. In contrast, Pil homologs are wide spread among nearly all cyanobacteria, both unicellular and filamentous, with the exception of a large clade of primarily marine unicellular picocyanobacteria.

Discussion

Several lines of evidence support the theory that Hps and Pil proteins compose the junctional pore complex, a T4P-like nanomotor that drives motility and polysaccharide secretion in *N. punctiforme*. First, most Hps and Pil proteins are essential for motility, consistent with the hypothesis that these proteins form a motor complex. Second, *hps*- and *pil*-deletion strains that lack motility either abolish or substantially decrease the secretion of hormogonium polysaccharide. Third, the subcellular localization of PilA, PilB, PilT1 and PilT2 places this system in rings at the cell poles adjacent to the septal junctions in motile hormogonia, which corresponds to the location of the JPC. Although our attempts to localize Hps proteins were largely unsuccessful, or in the case of HpsJ, did not localize to the septal junctions, it seems likely that, at minimum, the pseudopilin/minor pilin proteins, HpsB,C,D and H, are part of this complex given that most T4P and T2S systems described to date incorporate several minor pilins or pseudopilins, respectively (Peabody *et al*., 2003), and the *hps*-locus encodes the only minor pilin-/psuedopilin-like proteins in the *N. punctiforme* genome.

The results from immunofluorescent assays of PilA in the wild-type and various *pil*-deletion strains support a standard model for the function of these Pil homologs in the JPC. The requirement of PilB and PilQ for expression of PilA on the cell surface is consistent with roles as the pilus extension ATPase and outer membrane secretin, respectively, and the over-accumulation of PilA on the cell surface in the absence of PilT1 is consistent with a role for PilT1 as the pilus retraction ATPase. PilA monomers, possibly in combination with the pseudopilin/minor pilin proteins HpsB,C,D and H, most likely assemble a pilus-like structure on the outside of the cell, although, without more detailed ultrastructure data, we cannot make definitive statements about the existence and nature of these

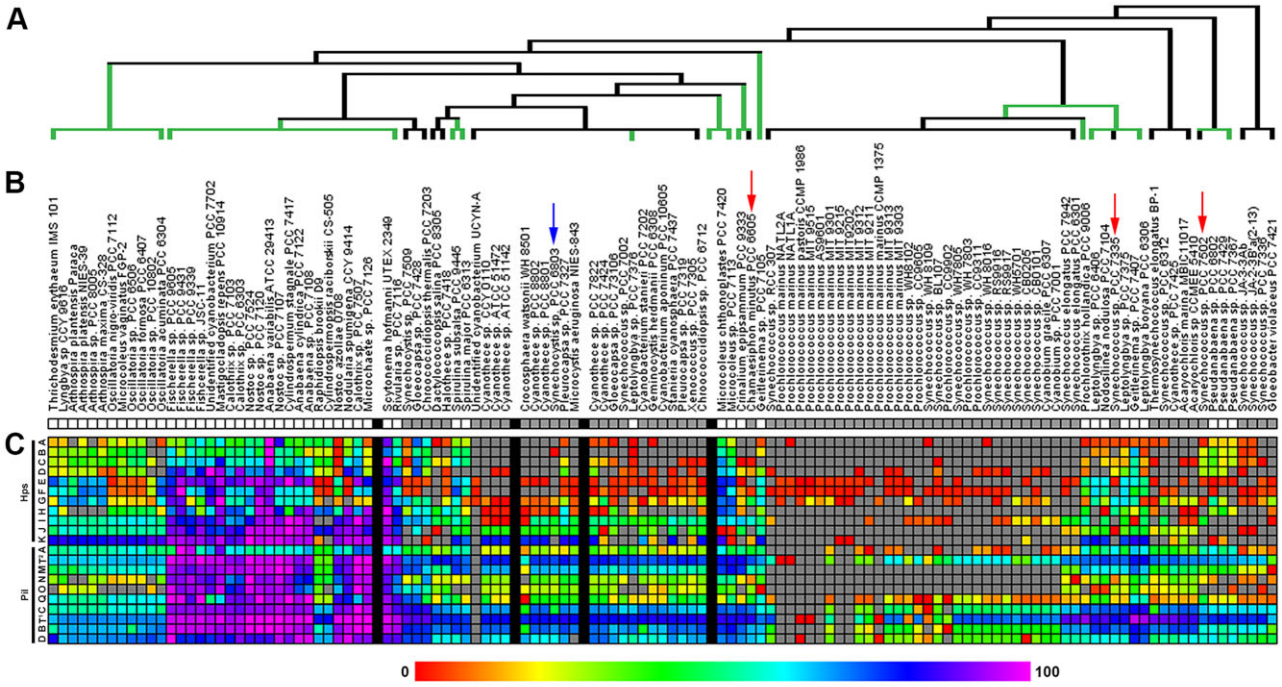

Fig. 6. Genomic conservation of Hps and Pil homologs in cyanobacteria.
A. Phylogenetic tree based on that reported by Shih *et al.* (2013). In the recent branches, green lines represent filamentous lineages, black lines unicellular.
B. Species names of cyanobacteria included in study and a heat map depicting whether strains are filamentous (white box) or unicellular (gray box). Black boxes represent strains in the phylogeny constructed by Shih *et al.* (2013) that were not included in this study. Red arrows indicate unicellular strains descendent from filamentous ancestors. Blue arrow indicates the model unicellular cyanobacterium *Synechocystis* sp. strain PCC 6803.
C. Heat map depicting blast scores for *N. punctiforme* Hps and Pil homologs (arranged based on order in the *N. punctiforme* genome) in other cyanobacteria. Each row represents the relative blast scores (scaled from near 0 for the lowest returned score to 100 for the highest returned score) for an Hps or Pil homolog (as indicated). Color values indicated by key, except for gray, which indicates no homolog was identified with a percent identity above 20%, the minimum cutoff for the IMG Genome Gene Best Homologs tool used in the study.

structures. The Hps proteins are dispensable for extension and retraction of PilA considering that *hps*-deletion strains neither lost nor over-accumulated surface PilA. Thus, the Hps proteins probably have a more specialized function in synthesis, secretion or interaction with the hormogonium polysaccharide.

The results from polysaccharide analysis of the wild-type and various *hps*- and *pil*-deletion strains is consistent with the JPC functioning as a polysaccharide secretion system. As depicted in Fig. 7, we propose a model where cycles of pilus extension and retraction, driven by the ATPases PilB and PilT1, respectively, translocate polysaccharide from the periplasm across the outermembrane through the channel formed by the secretin PilQ. This is supported by the facts that deletion of *pilB* or *pilQ* completely abolished secretion of hormogonium polysaccharide, whereas deletion of *pilT1* substantially reduced the secretion of the polysaccharide, despite the over accumulation of PilA on the cell surface. Alternatively, it is possible that hormogonium polysaccharide is secreted by a separate pathway which is co-ordinated to the activity of the T4P-system. This would be analogous to the regulation of extracellular polysaccharide (EPS) production in *M. xanthus*, which is controlled by a chemotaxis-like pathway that responds to the level of surface piliation (Black *et al.*, 2006). However, unlike *M. xanthus*, where inactivation of *pilT* increases the production of EPS due to hyperpiliation (Black *et al.*, 2006), the efficient secretion of hormogonium polysaccharide is dependent on both the pilus extension protein PilB and the pilus retraction protein PilT1. Therefore, if such a system exists, it must be co-ordinated to T4P activity in a different manner. Currently, we favor the former model as it is the most straightforward interpretation of the results and is consistent with historical observations that polysaccharide is secreted at the septal junction in other motile filamentous cyanobacteria (Walsby, 1968; Hoiczyk and Baumeister, 1998), although further work must be done to distinguish between these two possibilities.

The composition of the hormogonium polysaccharide is currently unknown. Previous reports by two groups found that hormogonia of *N. punctiforme* produce an RCA_{120}-

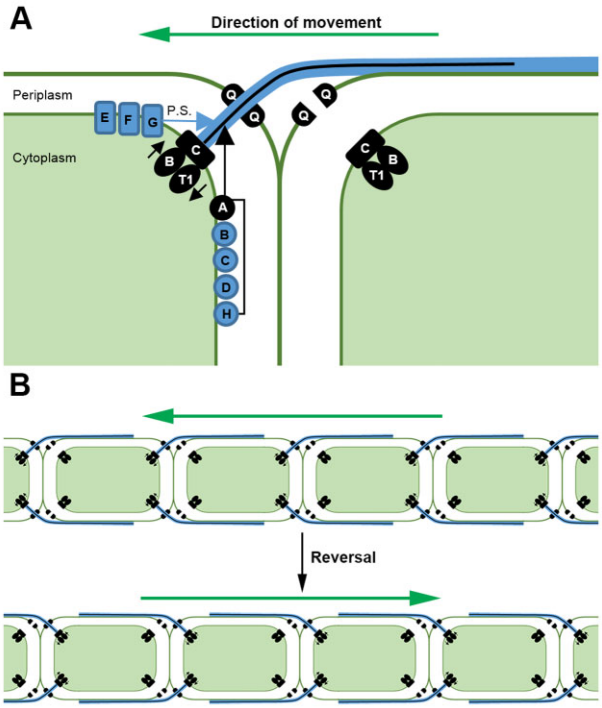

Fig. 7. A model of the JPC and gliding motility in filamentous cyanobacteria.
A. The hormogonium polysaccharide is synthesized by HpsE, F and G, and transported out of the periplasm through the pore formed by the secretin PilQ via cycles of pilus extension and retraction. The pilus is composed of PilA and possibly a combination of the minor/pseudopilins HpsB, C, D and H. The polysaccharide adheres tightly to the filament surface and continuous extension and retraction of the pilus translocates the polysaccharide along the length of the filament resulting in movement. PilC, which was not investigated in this study, is presumed to serve as an inner membrane platform for interaction with PilB and PilT1, as reported for other bacteria. Pil proteins and the pilus are black, Hps proteins and the hormogonium polysaccharide are blue. P.S. = polysaccharide. Arrows adjacent to PilB and PilT1 represent their roles as the pilus extension and retraction ATPases respectively. Other Pil and Hps proteins not depicted here are likely involved in the process. Large green arrows represent the direction of motion if motility is facilitated by the pilus pushing on the polysaccharide during pilus extension. If motility is facilitated by pulling on the polysaccharide during pilus retraction instead, the direction of motion would be reversed (B). Cells within an individual hormogonium filament co-ordinate the activation of JPC's on one side of each cell. Upon reversal, the cells co-ordinate the activation of the JPC's at the opposite cell pole. How this co-ordinated activation is achieved is currently unknown but we speculate it may involve PilT2 (not shown).

specific polysaccharide, indicating the presence of galactose (Schüßler *et al.*, 1997; Risser and Meeks, 2013). However, in the results presented here, where hormogonia were subjected to constant agitation to facilitate dispersal, we found that wild-type hormogonia produce a UEA-specific polysaccharide, indicating the presence of fucose. Only the Δ*hpsJ* strain produced substantial amounts of the RCA_{120}-specific polysaccharide, indicating that the activity of HpsJ affects polysaccharide composition. Whether HpsJ activity is constitutive, or dynamically modulates polysaccharide composition, perhaps in response to environmental conditions, is an intriguing question that requires further study. The glycosyl transferases HpsE, F and G most likely assemble at least part of the hormogonium polysaccharide, but are otherwise dispensable for motility, based on the observation that conditioned medium containing either UEA- or RCA_{120}-specific polysaccharides can restore motility in the Δ*hpsE-G* strain. This result implies that transport of the polysaccharide out of the cell is not a prerequisite for motility and, thus, does not support the theory that secretion of polysaccharide provides the motive force for gliding. Alternatively, it is conceivable that polysaccharide can be taken back into the cell and re-secreted. Considering the ability of T4P to import large polymers of DNA into cells, this does not seem out of the question (Averhoff and Friedrich, 2003).

If polysaccharide does not provide the thrust for motility, what role does it play? It may serve as an anchor for pilus retraction and/or facilitate interactions between PilA and the cell surface as in other systems. As determined by immunofluorescence assays, for the wild-type strain and mutant derivatives that retain motility, PilA adheres tightly to the surface of hormogonia. In contrast, PilA extends out and away from the surface of hormogonia in the Δ*hpsA*, Δ*hpsB-D* and Δ*hpsE-G* strains, which either produce low levels of polysaccharide or none at all. This observation is consistent with a role for hormogonium polysaccharide and possibly some combination of HpsA, and HpsB-D in facilitating an association between PilA and the cell surface. This close association may explain why pilus-like structures have not been observed for other motile filamentous cyanobacteria, despite the presence of T4P-like homologs encoded in their genomes. It is possible that pili extend out from the septal junctions and run parallel to the long axis of filaments in tight association with the cell surface. We speculate that some of the arrays of parallel fibers observed on or below the outer membrane of filamentous cyanobacteria in previous studies (Halfen and Castenholz, 1970; Hoiczyk and Baumeister, 1995; Adams *et al.*, 1998; Read *et al.*, 2007) may in fact be parallel arrays of pili. The interaction between the hormogonium polysaccharide and the cell surface may be facilitated by proteins present on the cell surface such as oscillin or s-layer proteins (Hoiczyk and Baumeister, 1995; 1997).

Based on these results, it is most likely that the motive force for gliding is produced by translocation of polysaccharide along the long axis of filaments via extension and retraction of a pilus-like structure. This could be accomplished by pulling on the polysaccharide as the pilus retracts, in a manner analogous to twitching motility or by pushing on the polysaccharide as the pilus extends. The latter model would be more compatible with the idea that

the junctional pores are also the site of polysaccharide secretion. In this scenario, polysaccharide is secreted out of the pores as the pilus extends, and interaction between the polysaccharide and the cell surface confine the motion of the polysaccharide laterally along the filament. If the polysaccharide remains fixed to the substratum, but is free to move laterally along the filament, this would result in movement. This model requires that the hormogonium polysaccharide not be anchored tightly to the filament the way it is in other twitching motility systems and is consistent with the fact that the majority of the polysaccharide either remains only loosely associated with the filaments, or dissolves into the medium for hormogonia in liquid suspension. Importantly, both of these models can account for the fact that exogenous addition of hormogonium-derived polysaccharide can complement a polysaccharide deficient mutant strain, because the motive force is not generated by secretion itself, but rather by the action of the pilus moving polysaccharide along the length of the filament. The question of whether pushing or pulling by the pilus ultimately generates the motive force could be answered by observation of PilA in motile filaments. If the pilus is pushing the polysaccharide, PilA should accumulate to the lagging side of septal junctions, while pulling would predict that PilA would accumulate to the leading side of septal junctions. Thus far, we have been unable to design an experiment that allows for observation of PilA either by live-cell immunofluorescence or labeling with protein specific fluorescent dyes, as described by Skerker and Berg (2001). The latter results in very high levels of staining over the entire cell and also renders hormogonia non-motile.

Presumably, efficient motility in a multicellular filament requires the co-ordinated activity of motors in all or most cells (Fig. 7B). The co-ordinated polarity of PilA in both motile hormogonia and non-motile Δ*hpsA*, Δ*hpsB-D* and Δ*hpsE-G* strains supports this idea. Unlike *M. xanthus* (Bulyha *et al*., 2009) and *Synechocystis* (Schuergers *et al*., 2015), this polarity does not appear to be due to dynamic localization of PilB given that PilB-GFP maintains a static bipolar localization during hormogonium motility reversals. Perhaps PilB remains static at the poles, but one or both of the PilT homologs oscillate between the motors at opposite ends of the cells to control motor activation. Because the PilT1- and PilT2-GFP fusions were not functional, we cannot draw definitive conclusions about whether their localization is static or dynamic upon reversal. However, the phenotype of the Δ*pilT2* strain would be consistent with a role for PilT2 in the co-ordinated switching of motors. Hormogonia of the Δ*pilT2* strain are mostly non-motile, but occasionally non-motile filaments begin to move, or motile filaments cease moving. If motor activation at each cell pole within cells of a filament were to lose co-ordination and become stochastic in the absence of PilT2, then filaments might only achieve motility on the rare occasion that a majority of the cells in a filament spontaneously achieve co-ordinated polarity of motor activation. The loss of co-ordinated localization of PilA in the Δ*pilT2*-deletion strain is also consistent with this idea. It is worth mentioning, however, that the time it takes for a hormogonium reversal, at most a few seconds, is much shorter than the time, on average 80 s, it takes for PilT to relocate from opposite cell poles in other organisms. such as *M. xanthus* (Bulyha *et al*., 2009). Thus, relocalization of PilT2, if it does occur, is unlikely to act fast enough to account for the rapid reversal of hormogonia, unless its translocation is directed by active transport rather than relying on passive diffusion. Regardless of the mechanism, it seems apparent that some means exists to co-ordinate and rapidly switch activation of motors on either end of the cell in hormogonia resulting in directed (tactic) motility.

The high degree of conservation of Hps and Pil proteins in filamentous cyanobacteria, and the fact that junctional pores have been observed in many of these organisms, support the theory that filamentous cyanobacteria share a common gliding mechanism. The absence of genes encoding Hps proteins in most unicellular cyanobacteria indicates that the filamentous system is distinct from the T4P system of *Synechocystis*. The most divergent aspects of the two systems probably have to do with the structure of the pilus, and the nature and secretion of any motility associated polysaccharides, given the difference in the minor pilin/psuedopilins between unicellular and filamentous cyanobacteria, and the lack of homologs to the *hps*-locus encoded glycosyl transferases. According to the phylogeny reported by Shih *et al*. (2013) filamentous cyanobacteria are not monophyletic and the filamentous form is proposed to have independently arisen multiple times. If this phylogeny is correct, then the presence of Hps homologs in filamentous cyanobacteria is either the result of convergent evolution or horizontal gene transfer. Alternatively, it is possible that most extant cyanobacteria arose from a common filamentous ancestor. In this scenario, selective pressure to maintain the Hps homologs exists only for filamentous cyanobacteria. Reversion to the unicellular state would relieve this pressure resulting in the concomitant loss of these protein over time. Additional studies would need to be done to distinguish between these possibilities.

Experimental procedures

Strains and culture conditions

For a detailed description of the plasmids, strains, and oligonucleotides used in this study refer to Tables S2 and S3. *N. punctiforme* ATCC 29133 (strain UCD 154) and its derivatives were cultured in Allan and Arnon medium diluted fourfold

(AA/4), without supplementation of fixed nitrogen, as previously described (Campbell *et al.*, 2007), with the exception that 5 and 10 mM sucralose was added to liquid and solid medium, respectively, to inhibit hormogonium formation (Splitt and Risser, submitted for publication). For hormogonium induction, the equivalent of 30 μg ml^{-1} chlorophyll *a* (Chl *a*) of cell material from cultures at a Chl *a* concentration of 10–20 μg ml^{-1} was harvested at 2000 *g* for 3 min, washed two times with AA/4 and resuspended in 2 ml of fresh AA/4. For selective growth, the medium was supplemented with 50 μg ml^{-1} neomycin. *Escherichia coli* cultures were grown in lysogeny broth (LB) for liquid cultures or LB supplemented with 1.5% (w/v) agar for plates. Selective growth medium was supplemented with 50 μg ml^{-1} kanamycin, 50 μg ml^{-1} ampicillin and 10 μg ml^{-1} chloramphenicol.

Plasmid and strain construction

The primers used for plasmid construction are indicated in Tables S2 and S3. All constructs were sequenced to insure sequence fidelity.

For in frame deletion of genes, approximately 900 bp of flanking DNA on either side of the gene and the first and last three or four codons of each gene were amplified via overlap extension PCR and cloned into pRL278 (Cai and Wolk, 1990) as BamHI-SacI fragments using restriction sites introduced on the primers.

In order to construct a mobilizable suicide vector containing the superfolder variant of *gfp* (*sfgfp*), the *sfgfp* coding region was synthesized *de novo* (GeneWiz) in order to remove *Bam*HI and *Sac*I restriction sites present in the native *sfgfp*. This variant of *sfgfp* was then amplified via PCR and cloned into pSCR569 (Risser *et al.*, 2012), from which *gfpuv* was excised, as a SmaI-SpeI fragment using restriction sites introduced on the primers to create pDDR338.

For replacement of chromosomal alleles with C-terminal *gfp*-tagged variants, approximately 900 bp of DNA downstream of the stop codon were amplified via PCR and cloned into pSCR569 or pDDR338 for *gfpuv* or *sfgfp* respectively, as SpeI-SacI fragments using restriction sites introduced on the primers and partial digests with *Spe*I where applicable due to the presence of a second *Spe*I site. Approximately 900 bp of DNA upstream of the stop codon were then amplified via PCR and cloned into this plasmid as a BamHI-SmaI fragment using restriction sites introduced on the primers.

For replacement of the chromosomal allele of *hpsA* with an N-terminal *gfp*-tagged variant, *gfpuv* was first amplified from pSCR569 via overlap extension PCR in order to remove a *Xho*I restriction site from the *gfpuv* coding frame, and cloned into pRL278 as a XhoI-SpeI fragment using restriction sites introduced on the primers to create pDDR296. Approximately 900 bp of DNA upstream of the start codon of *hpsA* were then amplified via PCR and cloned into pDDR296 as a *BamHI-SmaI* fragment using restriction sites introduced on the primers. Subsequently, approximately 900 bp of DNA downstream of the *hpsA* start codon were amplified via PCR and cloned into this plasmid as an SpeI-SacI (SpeI-partial) fragment to create pDDR306.

Gene deletions and allelic replacements were performed as previously described (Risser and Meeks, 2013).

Motility assays

All plate and time lapse motility assays were repeated in triplicate. For plate motility assays, individual colonies cultured on AA/4 supplemented with 10 mM sucralose were transferred to AA/4, 0.5% Noble agar plates, incubated for 48 h then imaged. Colony spreading was quantified by measuring the surface area covered by colonies from images converted to threshold. Phototaxis assays were prepared in the same manner, except that the plate was covered by a sleeve composed of an inner layer of black felt and outer layer of aluminum foil so that only one end of the plate was exposed to the light source. For quantification of phototaxis assays, the area corresponding to the inoculating colony was bisected perpendicular to the direction of the light source and the surface area of cell material that migrated out of the colony toward or away from the light source was quantified from threshold images.

For time-lapse microscopy, 2 μl of liquid suspensions containing hormogonia were spotted onto the surface of AA/4, 0.5% Noble agar plates and immediately covered with a cover slip. Images were taken every 15 s for 30 min. The velocity of individual filaments was quantified using the automated motion tracking ImageJ plugin wrMTrck (Nussbaum-Krammer *et al.*, 2015) followed by manual curation of the data.

Conditioned medium complementation assays

Induction of horomogonia was performed as described above, with the exception that between 18 and 24 h post induction suspensions were mixed hourly by vigorous pipetting in order to disperse aggregates and maximize dissolution of the hormogonium polysaccharide. Twenty-four hours after induction, cultures were centrifuged for 3 min at 2000 *g*, the supernatant was collected and centrifuged a second time at 16 000 *g* for 5 min. Supernatant was collected and 10 μl spotted onto colonies of various strains patched from AA/4, 10 mM sucralose to AA/4, 0.5% Noble agar. Plates were left uncovered until the liquid absorbed, sealed and incubated under standard growth conditions for 72 h, then imaged. Excess supernatant was stored at 4°C. For quantification of colony spreading, the surface area covered only by filaments that had migrated out of the colony was measured from images converted to threshold.

Microscopy

Plate, time-lapse and conditioned medium complementation assays were imaged using a Leica MZ APO dissecting microscope equipped with a Leica DFC290 digital camera controlled by micromanager imaging software (Edelstein *et al.*, 2014) and quantified using ImageJ (NIH).

Immunofluorescent labeling of PilA and RCA_{120}- or UEA-fluorescein staining of hormogonium polysaccharide was performed as previously described (Risser and Meeks, 2013; Risser *et al.*, 2014). Images of cellular autofluorescence, fluorescently labeled PilA or hormogonium polysaccharide, and GFP-tagged proteins were acquired with a Leica DMIRE2 inverted fluorescence microscope using metamorph software

(Molecular Devices) and a Yokogawa CSU-X1 spinning disc confocal with a QuantEM: 5125C camera. Excitation and emission were as follows: 491 nm excitation and 525 (± 25) nm emission for fluorescently labeled PilA, RCA_{120}- and UEA-fluorescein, and sfGFP proteins; 405 nm excitation and 525 (± 25) nm emission for GFPuv labeled proteins; and 561 nm excitation and 605 (± 25.5) nm emission for cellular autofluorescence. Subsequent image analysis was performed using ImageJ. For quantification of PilA at septal junctions, the segmented line tool (30 pt) was used to draw a line bisecting the long axis of a filament and then used to generate plot profiles for cellular autofluorescence and PilA immunofluorescence. The raw data for these profiles was exported to Excel and combined. The septal junction was defined by the periodic minima in autofluorescence along the plot profile. The sum of the PilA immunofluorescence signal was calculated for the next five pixels (0.89 μm) adjacent to either side of the septal junction. An example analysis of the wild-type strain can be found in supplemental Dataset S1.

For PilB-GFP time-lapse microscopy assays, cells were imaged at 10 s intervals with a 200 ms exposure for autofluorescence and PilB-GFP fluorescence followed by 8 s of white light illumination between images. Plot profiles of PilB-GFP were generated as described above for PilA immunofluorescence, but with a 20 pt line.

Immunoblot analysis

Detection of PilA via immunoblot analysis was performed as previously described (Risser *et al*., 2014). For immunoblot analysis of GFP-tagged proteins, cell material equivalent to 30 μg of Chl *a* was harvested and stored at –20°C. Cell pellets were resuspended in 40 μl of lysozyme solution (10 mg ml^{-1} lysozyme, 10 mM Tris, 25 mM EDTA, pH 8.0) and incubated on ice for 30 min, after which 160 μl of 10% SDS was added and the samples were incubated at 100°C for 10 min to extract proteins. Cell debris was removed by centrifugation at 16 000 *g* for 5 min and the proteins were precipitated from the supernatant by the addition of 800 μl acetone followed by incubation on ice for 10 min, then centrifugation at 16 000 *g* for 5 min. The supernatant was discarded, the pellets were air dried and reconstituted in 50 μl 8% SDS. Eight μl of sample were used for immunoblot analysis following standard SDS-PAGE and immunoblot procedures with a 1:2000 dilution of a rabbit polyclonal α-GFP antibody (Santa Cruz Biotechnology) and a 1:20 000 dilution of an HRP-conjugated secondary antibody (Chemicon).

Lectin blot analysis

For lectin blot analysis, 100 μl of culture conditioned medium was vacuum blotted onto a nitrocellulose membrane, then dried at 55°C for 5 min. The membrane was blocked for 30 min in Carbo-Free blocking solution (Vector laboratories), followed by incubation with biotinylated RCA_{120} or UEA (Vector laboratories) at a concentration of 2 μg ml^{-1} for 1 h. The membrane was subsequently washed 3× with Tris-buffered saline (TBS) containing 0.1% Tween 20 (TBST), incubated for one hour in VECTASTAIN® ABC reagent (Vector laboratories), washed 3× with TBST, then once with TBS, and followed by the addition of Clarity™ Western ECL blotting substrate (Bio-Rad) for chemiluminescent detection. Quantification of the signal intensities was performed by calculating the area under the curve from plot profiles generated using ImageJ.

Comparative genomics analysis

Comparative genomics analysis was performed using the IMG Genome Gene Best Homologs tool (Markowitz *et al*., 2012), set to the lowest percent identity cutoff (20+) with *N. punctiforme* as a reference genome, to query each of 120 different cyanobacterial genomes with complete, partial, or draft sequences available in the database. This data was then used to assemble a database containing the bit score for the corresponding best hit homolog for each *N. punctiforme* protein in each of the cyanobacterial genomes (Dataset S2). To generate heat maps depicting the bit scores for each protein on the same scale, the corresponding bit scores for each set of Hps and Pil proteins were transformed to a scale from 0 to 100, with 0 representing the lowest bit score for a homolog that returned a positive score, and 100 representing the highest bit score (Dataset S3). This scaled dataset was then used to generate heat maps using genesis (Sturn *et al*., 2002).

Acknowledgements

We would like to thank the Lin-Cereghino lab for use of and assistance with their vacuum blotting module.

This work was supported, in part, by grant IOS 08222008 from the US National Science Foundation to JCM.

References

Adams, D.G. (2001) How do cyanobacteria glide? *Microbiology Today* **28:** 131–133.

Adams, D.G., Ashworth, D., and Nelmes, B. (1998) Fibrillar array in the cell wall of a gliding filamentous cyanobacterium. *J Bacteriol* **181:** 884–892.

Averhoff, B., and Friedrich, A. (2003) Type IV pili-related natural transformation systems: DNA transport in mesophilic and thermophilic bacteria. *Arch Microbiol* **180:** 385–393.

Bhaya, D., Bianco, N.R., Bryant, D., and Grossman, A. (2000) Type IV pilus biogenesis and motility in the cyanobacterium *Synechocystis* sp. PCC6803. *Mol Microbiol* **37:** 941–951.

Black, W.P., Xu, Q., and Yang, Z. (2006) Type IV pili function upstream of the *dif* chemotaxis pathway in *Myxococcus xanthus* EPS regulation. *Mol Microbiol* **61:** 447–456.

Bulyha, I., Schmidt, C., Lenz, P., Jakovljevic, V., Hone, A., Maier, B., *et al*. (2009) Regulation of the type IV pili molecular machine by dynamic localization of two motor proteins. *Mol Microbiol* **74:** 691–706.

Cai, Y.P., and Wolk, C.P. (1990) Use of a conditionally lethal gene in *Anabaena* sp. strain PCC 7120 to select for double recombinants and to entrap insertion sequences. *J Bacteriol* **172:** 3138–3145.

Campbell, E.L., Summers, M.L., Christman, H., Martin, M.E.,

and Meeks, J.C. (2007) Global gene expression patterns of *Nostoc punctiforme* in steady-state dinitrogen-grown heterocyst-containing cultures and at single time points during the differentiation of akinetes and hormogonia. *J Bacteriol* **189:** 5247–5256.

Campbell, E.L., Hagen, K.D., Chen, R., Risser, D.D., Ferreira, D.P., and Meeks, J.C. (2015) Genetic analysis reveals the identity of the photoreceptor for phototaxis in hormogonium filaments of *Nostoc punctiforme*. *J Bacteriol* **197:** 782–791.

Castenholz, R.W. (1982) Motility and taxis. In *The Biology of Cyanobacteria*. Carr, N.G., and Whitton, B.A. (eds). Oxford: Blackwell scientific publications, pp. 413–419.

Damerval, T., Guglielmi, G., Houmard, J., and De Marsac, N.T. (1991) Hormogonium differentiation in the cyanobacterium *Calothrix*: a photoregulated developmental process. *Plant Cell* **3:** 191–201.

Dhahri, S., Ramonda, M., and Marliere, C. (2013) In-situ determination of the mechanical properties of gliding or non-motile bacteria by atomic force microscopy under physiological conditions without immobilization. *PLoS ONE* **8:** e61663.

Dick, H., and Stewart, W.D.P. (1980) The occurrence of fimbriae on a N_2-fixing cyanobacterium which occurs in lichen symbiosis. *Arch Microbiol* **124:** 107–109.

Duggan, P.S., Gottardello, P., and Adams, D.G. (2007) Molecular analysis of genes in *Nostoc punctiforme* involved in pilus biogenesis and plant infection. *J Bacteriol* **189:** 4547–4551.

Edelstein, A.D., Tsuchida, M.A., Amodaj, N., Pinkard, H., Vale, R.D., and Stuurman, N. (2014) Advanced methods of microscope control using μManager software. *J Biol Methods* **1:** e10.

Giltner, C.L., Nguyen, Y., and Burrows, L.L. (2012) Type IV pilin proteins: versatile molecular modules. *Microbiol Mol Biol Rev* **76:** 740–772.

Halfen, L.N., and Castenholz, R.W. (1970) Gliding in a blue-green alga: a possible mechanism. *Nature* **225:** 1163–1165.

Hoiczyk, E., and Baumeister, W. (1995) Envelope structure of four gliding filamentous cyanobacteria. *J Bacteriol* **177:** 2387–2395.

Hoiczyk, E., and Baumeister, W. (1997) Oscillin, an extracellular, Ca^{2+}-binding glycoprotein essential for the gliding motility of cyanobacteria. *Mol Microbiol* **26:** 699–708.

Hoiczyk, E., and Baumeister, W. (1998) The junctional pore complex, a prokaryotic secretion organelle, is the molecular motor underlying gliding motility in cyanobacteria. *Curr Biol* **8:** 1161–1168.

Jarrell, K.F., and McBride, M.J. (2008) The surprisingly diverse ways that prokaryotes move. *Nat Rev Microbiol* **6:** 466–476.

Kluge, M., Mollenhauer, D., and Wolf, E. (2003) The *Nostoc-Geosiphon* endocytobiosis. In *Cyanobacteria in Symbiosis*. Rai, A.R., Bergman, B., and Rasmussen, U. (eds). Dordrecht: Springer, pp. 19–30.

Li, Y., Sun, H., Ma, X., Lu, A., Lux, R., Zusman, D., and Shi, W. (2003) Extracellular polysaccharides mediate pilus retraction during social motility of *Myxococcus xanthus*. *Proc Natl Acad Sci USA* **100:** 5443–5448.

Markowitz, V.M., Chen, I.M., Palaniappan, K., Chu, K., Szeto, E., Grechkin, Y., *et al*. (2012) IMG: the integrated microbial genomes database and comparative analysis system. *Nucleic Acids Res* **40:** D115–D122.

Meeks, J.C. (2006) Molecular mechanisms in the nitrogen-fixing *Nostoc*-Bryophyte symbiosis. *Prog Mol Subcell Biol* **41:** 165–196.

Melville, S., and Craig, L. (2013) Type IV pili in gram-positive bacteria. *Microbiol Mol Biol Rev* **77:** 323–341.

Merz, A.J., So, M., and Sheetz, M.P. (2000) Pilus retraction powers bacterial twitching motility. *Nature* **407:** 98–102.

Nussbaum-Krammer, C.I., Neto, M.F., Brielmann, R.M., Pedersen, J.S., and Morimoto, R.I. (2015) Investigating the spreading and toxicity of prion-like proteins using the metazoan model organism C. elegans. *J Vis Exp* 52321. doi: 10.3791/52321

Peabody, C.R., Chung, Y.J., Yen, M.R., Vidal-Ingigliardi, D., Pugsley, A.P., and Saier, M.H., Jr (2003) Type II protein secretion and its relationship to bacterial type IV pili and archaeal flagella. *Microbiology* **149:** 3051–3072.

Read, N., Connell, S., and Adams, D.G. (2007) Nanoscale visualization of a fibrillar array in the cell wall of filamentous cyanobacteria and its implications for gliding motility. *J Bacteriol* **189:** 7361–7366.

Rippka, R., Castenholz, R.W., and Herdman, M. (2001) Oxygenic photosynthetic bacteria. subsection IV. In *Bergey's Manual of Systematic Bacteriology*. Boone, D.R., Castenholz, R.W., and Garrity, G.M. (eds). New York: Springer, pp. 562–589.

Risser, D.D., and Callahan, S.M. (2009) Genetic and cytological evidence that heterocyst patterning is regulated by inhibitor gradients that promote activator decay. *Proc Natl Acad Sci USA* **106:** 19884–19888.

Risser, D.D., and Meeks, J.C. (2013) Comparative transcriptomics with a motility-deficient mutant leads to identification of a novel polysaccharide secretion system in *Nostoc punctiforme*. *Mol Microbiol* **87:** 884–893.

Risser, D.D., Wong, F.C., and Meeks, J.C. (2012) Biased inheritance of the protein PatN frees vegetative cells to initiate patterned heterocyst differentiation. *Proc Natl Acad Sci USA* **109:** 15342–15347.

Risser, D.D., Chew, W.G., and Meeks, J.C. (2014) Genetic characterization of the *hmp* locus, a chemotaxis-like gene cluster that regulates hormogonium development and motility in *Nostoc punctiforme*. *Mol Microbiol* **92:** 222–233.

Schuergers, N., Nurnberg, D.J., Wallner, T., Mullineaux, C.W., and Wilde, A. (2015) PilB localization correlates with the direction of twitching motility in the cyanobacterium *Synechocystis* sp. PCC 6803. *Microbiology* **161:** 960–966.

Schüßler, A., Meyer, T., Gehrig, H., and Kluge, M. (1997) Variations of lectin binding sites in extracellular glycoconjugates during the life cycle of *Nostoc punctiforme*, a potentially endosymbiotic cyanobacterium. *Eur J Phycol* **32:** 233–239.

Shepard, R.N., and Sumner, D.Y. (2010) Undirected motility of filamentous cyanobacteria produces reticulate mats. *Geobiology* **8:** 179–190.

Shih, P.M., Wu, D., Latifi, A., Axen, S.D., Fewer, D.P., Talla, E., *et al*. (2013) Improving the coverage of the cyanobac-

terial phylum using diversity-driven genome sequencing. *Proc Natl Acad Sci USA* **110:** 1053–1058.
Skerker, J.M., and Berg, H.C. (2001) Direct observation of extension and retraction of type IV pili. *Proc Natl Acad Sci USA* **98:** 6901–6904.
Sturn, A., Quackenbush, J., and Trajanoski, Z. (2002) Genesis: cluster analysis of microarray data. *Bioinformatics* **18:** 207–208.
Walsby, A.E. (1968) Mucilage secretion and the movement of blue-green algae. *Protoplasma* **65:** 223–238.

Supporting information

Additional supporting information may be found in the online version of this article at the publisher's web-site.